Interference-Aware Topology Control for Low Rate Wireless Personal Area Networks

Junseok KIM, *Nonmember* and Younggoo Kwon, *Member*, IEEE

Abstract — *The topology control technique can prolong the network lifetime, but it can suffer the significant performance degradation due to the interferences of WLAN or Bluetooth devices. This paper proposes an interference-aware topology control algorithm to reduce the interference effects. The basic idea of the proposed algorithm is to estimate the interference effects exactly and re-construct the robust network topology to the interference variations. From experimental results, we confirm that the proposed algorithm outperforms the previous algorithms in terms of the delivery and energy performance.* [1]

Index Terms — Interference-Aware, Topology Control, Low-Rate Wireless Personal Area Network, ZigBee, IEEE 802.15.4

I. INTRODUCTION

The development of wireless technologies will change the way of controlling elements in smart home systems. The IEEE 802.15.4/ZigBee is the standard for residential and industrial applications in the low-rate wireless personal area networks (LR-WPANs) [1][2]. The LR-WPAN nodes will be placed in homes or factories, and communicate wirelessly to monitor and control various application devices. The topology control is one of the most effective power-saving techniques in LR-WPANs [5]. The topology control tries to remove the long distance links and uses the minimum transmit power to reduce the energy consumptions. Topology control algorithms use the location information with the GPS at each node [6-8], while a few algorithms use the signal attenuation or the packet reception ratio as the link costs for the topology construction [9-13]. The LR-WPAN uses the 2.4GHz ISM band and this band is heavily crowded by the wireless LAN (WLAN) and Bluetooth devices. Experimental results have shown that the LR-WPAN can suffer the significant performance degradation due to the interference effects [14][15]. Under the topology control algorithms without considering the interference, the LR-WPAN packets can be corrupted easily by the interference. The adaptive frequency hopping algorithm or the channel selection algorithms are proposed to avoid the interference problems [16-19].

In this paper, we propose a novel topology control algorithm for the LR-WPAN, namely, the interference-aware topology control (ITC) algorithm. In the proposed algorithm, each node estimates the interference effects periodically and determines the minimum transmit power. The minimum transmit power is used as the link cost for constructing the network topology. If the interference is detected, the proposed algorithm tries to find the new paths locally which can detour the interference region. To reduce the temporal interference variations, the proposed algorithm compensates the minimum transmit power with the margin. The cooperation with the routing algorithm is also considered. We evaluate the performance of the proposed algorithm with the simulations and the real testbed experiments. The performance results show that the proposed algorithm outperforms the previous algorithms in terms of the delivery ratio and the energy consumption in the presence of the interferences.

The rest of this paper is organized as follows. In the next section, we describe the related works. In section III, we present the procedure for estimating the minimum transmit power with the interference effect analysis. In section IV, we propose the interference aware topology control algorithm. The performance evaluation is carried out in section V. In the final section, we present the conclusions.

II. RELATED WORKS

Many researchers have been investigated the interference effects on the LR-WPANs [10][11]. The WLAN is the dominant interference source because it uses the wider channel (20MHz) and the higher transmit power (100mW) than the LR-WPANs [11]. To minimize the WLAN interference effects, the dynamic channel selection algorithms are introduced [11][12]. In these algorithms, the frequency channels are scanned periodically and the base-station selects the frequency channel which has little interference effects. The dynamic channel selection can improve the network performance. However, there are still problems because all frequency channels could be occupied. The IEEE 802.11 draft N uses 40MHz channel bandwidth, that is, all 2.4GHz ISM band could be occupied by the two sets of the WLAN products [14]. In addition, the dynamic channel selection can cause the large networking overheads if the wireless devices move around.

The origin of the topology control is the proximity graphs in the theory of computational geometry such as the Gabriel Graph (GG) and the Relative Neighbor Graph (RNG) [5]. Let $G = (V, E)$ denote the graph without the topology control where V and E are the vertex set and the edge set in the network. Let $G_{TC} = (V, E_{TC})$ be the graph with the topology control where E_{TC} is the set of remaining edges. Among the proximity graphs, the RNG has good properties for the topology control and the routing protocol in the ad-hoc networks [8]. Let $c(u, v)$ be the cost of the edge (u, v). The topology of the RNG is defined as $G_{RNG}=(V, E_{RNG})$ where $(u,$

---

[1] This paper was supported by Konkuk University in 2008.

The authors are with the Department of Electronic Engineering, Konkuk University, 1 Hwayang-dong, Gwangjin-gu, Seoul 143-701, Korea. (email: {jskim1, ygkwon}@konkuk.ac.kr)

$v) \in E_{RNG}$ *if and only if* $c(u, v) < c(u, w) \wedge c(v, u) < c(v, w)$ *for* $\exists w \in V$. That is, in the RNG, as shown in Fig. 1-(a), the lune does not contain any other node, where lune denotes the overlapped region of the node *u*, *v* transmission range.

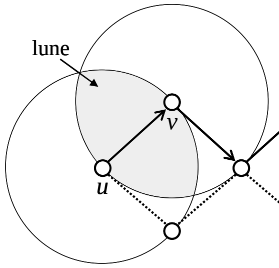

(a) RNG

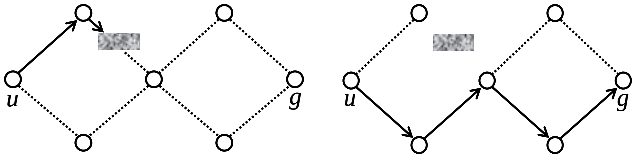

(b) disadvantage of RNG (c) XTC

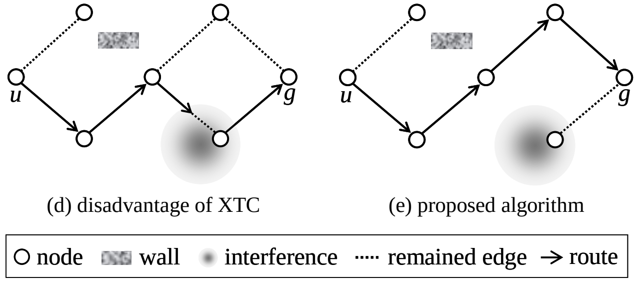

(d) disadvantage of XTC (e) proposed algorithm

Fig. 1. Topology control examples

Generally, the cost of the edge is defined by the Euclidean distance. However, this distance based RNG can fail to deliver the message under the obstacle environments which is shown in Fig. 1-(b). To remove this problem, the XTC uses the signal attenuation as the cost of the edge to constructs the RNG [7]. However, the signal attenuation could not provide the exact interference effects. The XTC can fail to deliver the messages when there are various interference effects.

III. MINIMUM TRANSMIT POWER WITH CONSIDERING INTERFERENCE EFFECTS

A. Interference Effect Analysis

We measure the WLAN interference power by using the LR-WPAN (MTM-CM3000) device under difference applications with the WLAN (N200UA) devices. The MTM-CM3000 has the CC2420 IEEE 802.15.4(2003) radio [17] and the N200UA has the RT2870 IEEE 802.11a/b/g/n radio [18]. We use the TITANIS omni-directional antenna on both devices [19]. We define the interference-occupy-ratio γ as follows:

$$\gamma = n / N \qquad (1)$$

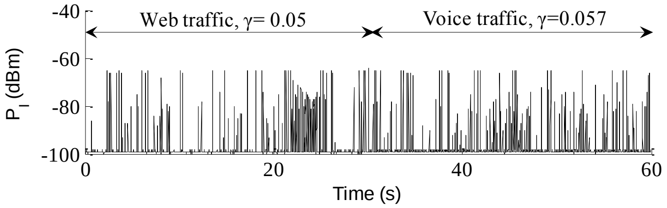

(a) low-traffic-rate WLAN interference

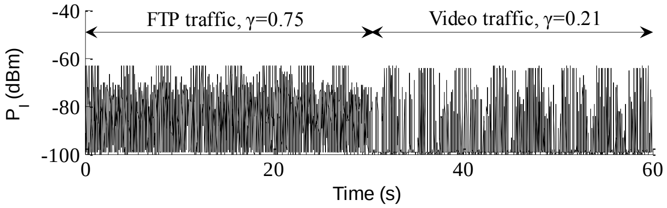

(b) high-traffic-rate WLAN interference

Fig. 2. Measured interference power P_I and interference-occupy-ratio γ

where n denotes the number of detecting the interference over *N* samples. Fig. 2-(a) shows the WLAN interference power under the web and voice traffic applications. Since the channel is not heavily occupied, the LR-WPAN can transmit the message through the intervals. Fig. 2-(b) shows the interference power under the file transfer protocol (FTP) and the voice traffic applications. Since the channel is heavily occupied, the packet transmission of LR-WPAN is corrupted easily by WLAN interference.

The topology control algorithms construct the topology based on the link quality parameters such as the distance or the signal attenuation. The IEEE 802.15.4 standard defines two link quality estimators: the link-quality-indication (LQI) and the received-signal-strength-indicator (RSSI) [1]. The LQI is the average correlation value of 8 symbols (4-bytes) after the start of a packet. The RSSI is the average signal strength over 8 symbol periods (128*us*). We conducted experiments with real wireless products to investigate the interference effect on the link quality estimators. In the experiments, one LR-WPAN node transmits 200 50-byte messages at different transmit power levels (-20 to 0dBm) at the rate of 10 packets per second. The other LR-WPAN node records the packet reception ratio (PRR), RSSI, LQI, and the interference power values. In the meanwhile, one WLAN node downloads a big file from the other WLAN node through the FTP application to generate the -75dBm interference to the LR-WPAN nodes.

Fig. 3 shows the correlation between the PRR and the link quality estimators. The LQI has large variations over time as shown in Fig. 3-(a). The RSSI has relatively small variations than the LQI and has strong correlation with the PRR as shown in Fig. 3-(b). However, the RSSI threshold is affected much by the interference effects. As shown in Fig. 3-(c), the signal-to-interference-plus-noise ratio (SINR) shows a strong correlation regardless of the interference effects and it has relatively small variations. From the experimental results, we observe that the SINR can be used as a good link quality estimator regardless of the interference effects.

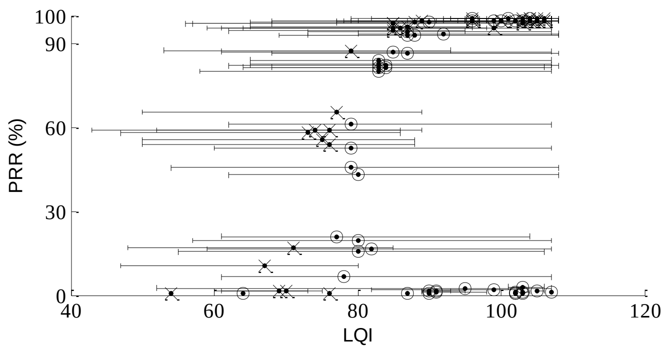

(a) PRR vs. LQI

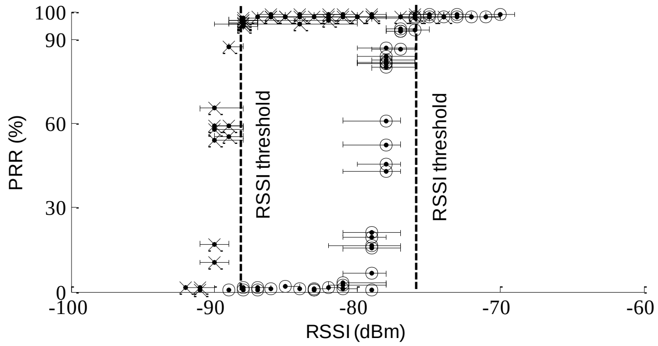

(b) PRR vs. RSSI

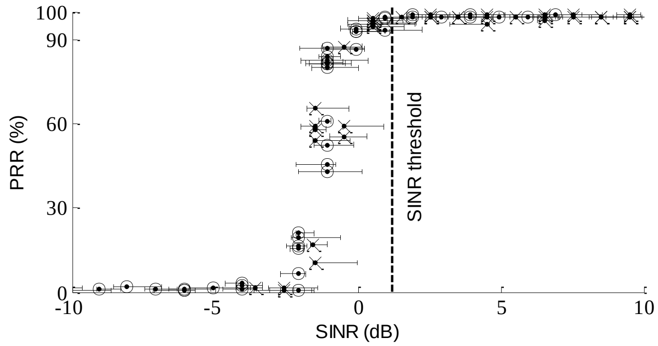

(c) PRR vs. SINR

Fig. 3. Interference effects on link quality estimators

B. Interference-aware minimum transmit power estimation

The topology control protocol determines the minimum transmit power to reduce the energy consumption and to increase the channel capacity [5]. However, the minimum transmit power based on the distance or the RSSI value is vulnerable to the interference effects. In this paper, we derive the minimum transmit power based on the SINR value.

As shown in Fig. 3, the PRR is close to 100% when the received power (= RSSI) is above a certain threshold, but the threshold is affected by the interference. If we know the proper received-power-threshold at a certain interference power, the minimum-transmit-power, P_{TX}^{MIN}, is determined as follows:

$$P_{TX}^{MIN}(dBm) = PL(dB) + P_{RX}^{TH}(dBm) \qquad (2)$$

where PL and P_{RX}^{TH} denote the path loss and the received power threshold. The path loss is the power reduction of the signal between the sender and the receiver due to the distance and obstacles. We can obtain the path loss by subtracting the transmitted power from the received power [22].

As shown in Fig. 3-(c), the SINR threshold is not affected much by the interference effects. The SINR is the power ratio between the strength of the desired signal to the strength of the undesired signals.

$$SINR(dB) = 10\log\frac{10^{P_{RX}/10}}{10^{P_I/10} + 10^{P_N/10}} \qquad (3)$$

where P_{RX}, P_I, and P_N denote the received power, the interference power, and the noise power respectively (in dBm). We rearrange (3) as follows:

$$P_{RX} = 10\log\left(10^{P_N/10} + 10^{SINR/10} \times 10^{P_I/10}\right) \qquad (4)$$

If we know the noise and the interference power, we can derive the received-power-threshold that provides a certain SINR target. In the IEEE 802.15.4 standard, the bit error ratio (BER) is determined by the SINR as follows [1]:

$$BER = \frac{8}{15} \times \frac{1}{16} \times \sum_{k=2}^{16}\left[-1^{k}\binom{16}{k} e^{\left(20\times SINR\times\left(\frac{1}{k}-1\right)\right)}\right] \qquad (5)$$

Reversely, we can determine the SINR target that satisfies a certain BER target. We set the SINR target as 1.01dB to provide 99% PRR with 100 bytes packet.

The noise power depends on the hardware [21]. The interference power can be measured by reading the RSSI register of the radio [21]. We can distinguish the interference signal from the IEEE 802.15.4 signal by checking the start of the frame delimiter (SFD) pin (i.e., the SFD pin goes high when the radio receives the IEEE 802.15.4 signal [23]).

Now, the minimum transmit power is obtained as follows:

$$P_{TX}^{MIN} = P_{RX} - P_{TX}^{old} + 10\log\left(10^{P_N/10} + 1.29\times 10^{P_I/10}\right) \qquad (6)$$

where P_{TX}^{old} is the old transmitted power (i.e., previous transmit power). Note that this minimum transmit power depends on the effects of the distance, the obstacles, and the interferences at the same time. The proposed algorithm will use this minimum transmit power as the link cost for the topology control.

IV. PROPOSED ALGORITHM

The basic idea of the proposed algorithm is to adaptively avoid the routes which are affected by the interferences in the topology construction. In the proposed algorithm, each node estimates the interference effects periodically and determines the minimum transmit power for its neighbors. Each node constructs the topology by removing or detouring the links which are severely affected by the interferences.

A. *Interference Effect Estimation*

The LR-WPAN radio such as CC2420 can measure the signal strength by reading the RSSI register [21]. When it begins to receive the LR-WPAN message, the SFD pin of the radio goes high [23]. When the RSSI value is above the noise power and the SFD pin is low, the measured signal strength is the interference power. We assume that the LR-WPAN uses the duty-cycling technique to reduce the power consumption (i.e., it wakes up and sleep periodically).

In the proposed algorithm, as shown in Fig. 4, each node reads the RSSI register at the start of every wake-up period for a short time (it takes 128*us*). For every 50 wake-up periods, each node estimates the interference-occupy-ratio, γ, by using (1). When the wireless channel is occupied heavily by the interference (i.e., $\gamma > 0.20$ from Fig. 2), the node estimates the received power threshold by using (4). When the wireless channel is not occupied heavily, the node uses the default received power threshold. We set the default received power threshold as -94dBm from [23]. If the received power threshold is changed by δ, the node broadcasts the received power threshold value by using the maximum transmit power. Since δ should be larger than the standard deviation of the interference power, we set δ as 10dB from the empirical measurements [22].

When the node *u* received the received power threshold value from the node *w*, it measures the received signal power and estimates the path loss as follows:

$$PL(dB) = P_{RX}(dBm) - P_{TX}^{MAX}(dBm) \tag{7}$$

where *PL* denotes the path loss. Then, the node *u* can determine the minimum transmit power for the node *w*, ${}^{u\to w}P_{TX}^{MIN}$, by using (2).

B. *Topology Management*

After the node *u* estimates the minimum transmit power values for all neighbors, it establishes the neighbor minimum transmit power list in ascending order and broadcasts the neighbor list. After the node *u* received the neighbor lists from all neighbors, it constructs the local topology. Let ${}^{u}G_{ITC} = ({}^{u}V_{ITC}, {}^{u}E_{ITC})$ be the local topology of the node *u*, where ${}^{u}V_{ITC}$ is the neighbor list of the node *u*. The edge set, ${}^{u}E_{ITC}$, is defined as follows:

$$(u, v) \in {}^{u}E_{ITC} \ \textit{if and only if (iif)} \quad {}^{u\to v}P_{TX}^{MIN} < {}^{u\to w}P_{TX}^{MIN} \wedge {}^{v\to u}P_{TX}^{MIN} < {}^{v\to w}P_{TX}^{MIN} \ \textit{for} \exists w \in {}^{u}V_{ITC} \tag{8}$$

As we stated, the proposed algorithm periodically estimates the interference effect and adjusts the minimum transmit power. If a value of the minimum transmit power is changed in the interference region, the affected nodes and its neighbors re-construct their local topologies.

The neighbor list contains the addresses of the neighbor nodes to reduce the message overhead. For example, in Fig. 6-(a), the neighbor list of the node *u* is {*w*, *v*}. When the node *w* is affected by the interference, the neighbor list of the node *u* is changed to {*v*, *w*}. Consequently, the edge (*u*, *v*) can be established because ${}^{u\to v}P_{TX}^{MIN} < {}^{u\to w}P_{TX}^{MIN}$ as shown in Fig. 6-(b). The minimum transmit power depends only on the distance when there is no obstacles and no interferences (i.e., free-space). In the free-space, the proposed algorithm constructs the same topology of the RNG as shown in Fig. 6-(a). When the node *w* is affected by the interference, the proposed algorithm changes the topology as shown in Fig. 6-(b). The proposed algorithm changes the route from $u \rightarrow w \rightarrow v$ to $u \rightarrow v$ by cooperating with the routing protocol. Note that the node *u* cannot cut the edge (*u*, *v*) unless the edge (*u*, *w*) and (*w*, *v*) exist. That is, the proposed algorithm can preserve the network connectivity in the presence of the interferences.

$P_{TX}^{MAX(MIN)}$	maximum (or minimum) transmit power
$P_{RX}^{[TH]}$	received power [threshold]
γ	interference-occupy-ratio: *n* detecting interference over *N* samples
$P_{N(I)}$	noise (or interference) power

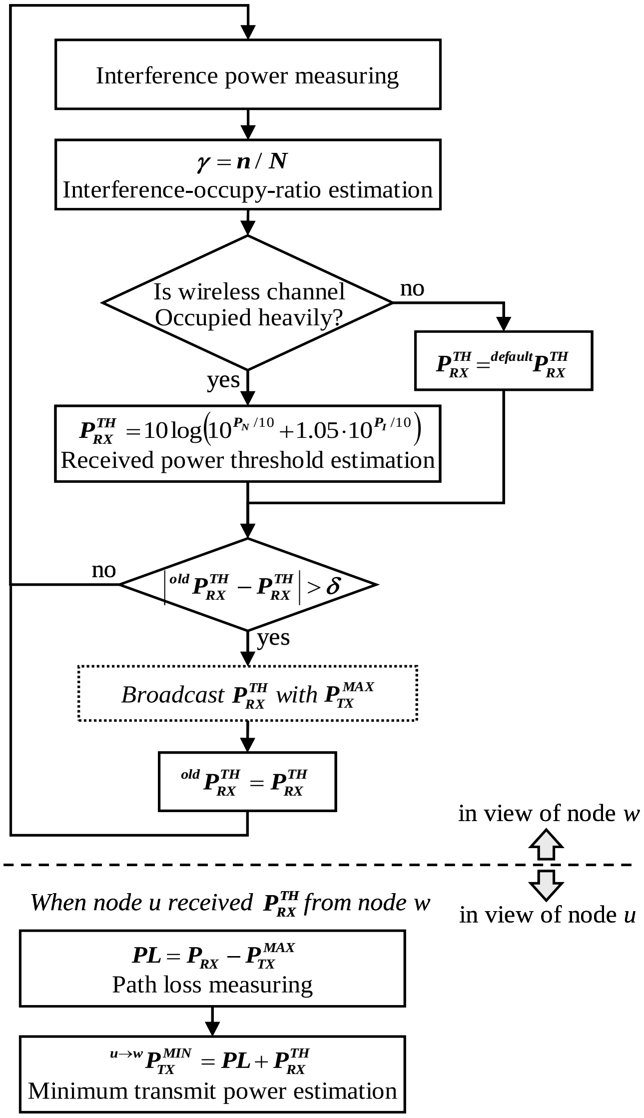

Fig. 4. Flowchart of interference effect estimation

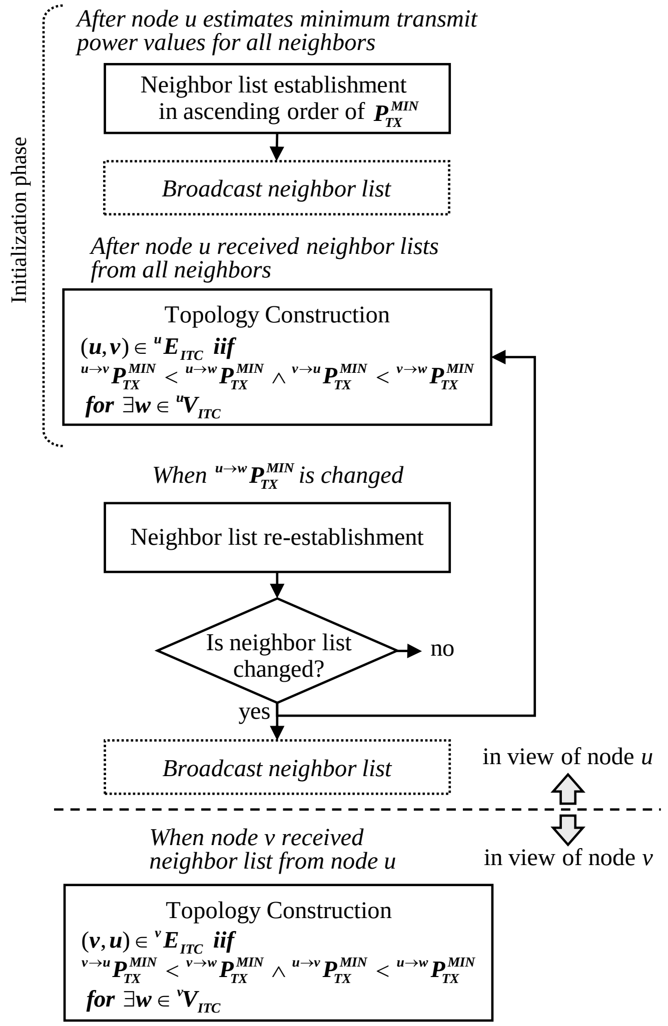

Fig. 5. Flowchart of topology management

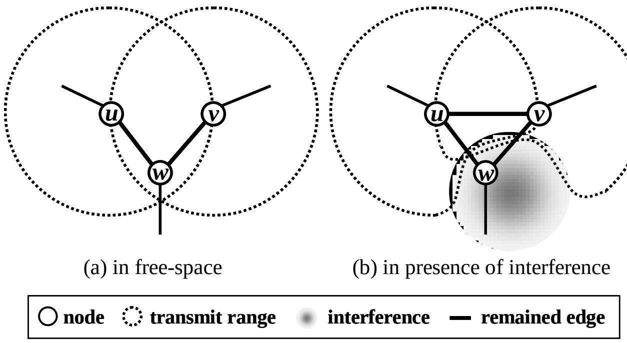

(a) in free-space (b) in presence of interference

Fig. 6. Constructed topology based on proposed algorithm

C. Practical Improvement

From the experiments, we observe that the interference power fluctuates much at times. Therefore, determining the minimum transmit power based on the analytical model could not be enough. To reduce the temporal interference effect variations, the proposed algorithm compensates the minimum transmit power with the margin as follows:

$$P_{TX} = P_{TX}^{MIN} + M \qquad (9)$$

- If packet in error: M += Δ.

- Else: M-= Δ/k, M>= 0.

where M is the margin. If a node notices that its packet transmission has failed possibly due to the interferences, the transmit power will be increased by *Δ*. The *Δ* increased transmit power can be returned to the minimum transmit power after *k* consecutive packet transmission successes. To maintain the steady margin, a packet transmission error needs to be followed after *k* consecutive packet transmission successes in order to maintain the steady margin. *k* is defined as *p*/(*1*-*p*), where *p* is the desired PRR target [20]. We set *k* as 19 to provide 95% PRR. We set *Δ* as 3dB because the maximum difference in nearby transmit power level is 2dB on CC2420 [23]. Note that we use the margin to keep a good link quality against the temporal interference variations, and the margin does not affect to the edge cost of the topology control.

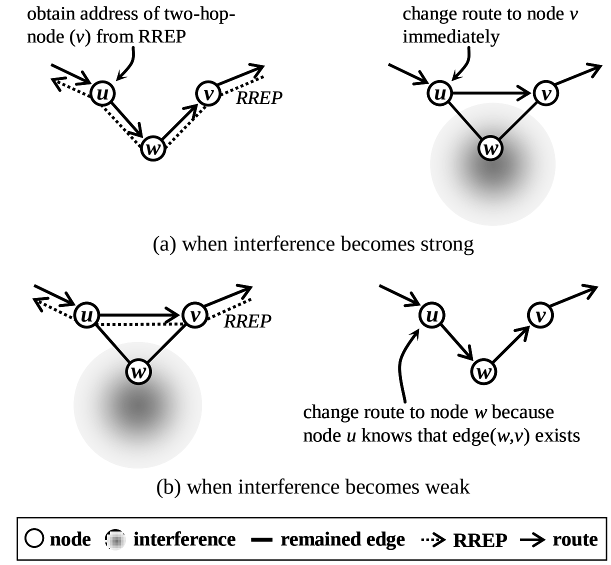

(a) when interference becomes strong

(b) when interference becomes weak

Fig. 7. Cooperation with routing protocol

The ZigBee standard, which specifies the network layer of the LR-WPANs, uses the ad-hoc on-demand distance vector (AODV *Jr.*) as the routing protocol [2]. To discover the route, the ZigBee routing protocol floods the route request (RREQ) messages. When the destination node received the RREQ message, it forwards the route reply (RREP) message back to the source node. When the route is broken, the intermediate node forwards the route error (RERR) message to the source node and the source node begins to flood the RREQ message again. To reduce routing overheads in the proposed algorithm, we modify the routing protocol by using the RREP with the two-hop node information. As shown in Fig. 7-(a), the node *u* knows that the node *v* is the two-hop neighbor on the route from the RREP. When the edge (*u*, *v*) is established due to the interference, the node *u* changes the route to the node *v* without the route recovery. In Fig. 7-(b), the node *u* removes the edge (*u*, *v*) when the interference disappears. From the topology management, the node *u* knows that the edge (*w*, *v*) exits. The topology control protocol of the node *u* informs the routing protocol to forward the message to the node *w*.

V. PERFORMANCE EVALUATIONS

A. *Simulation Results*

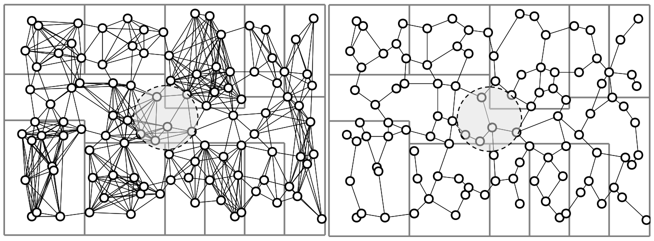

(a) without topology control (b) distance-based algorithm

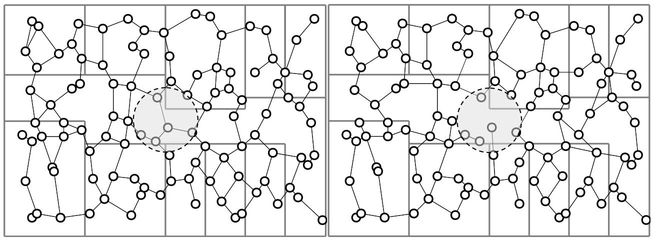

(c) RSSI-based algorithm (d) proposed algorithm

○ node ◌ interference — wall — remained edge

Fig. 8. Constructed topology based on different algorithms

We perform simulations to evaluate the performance of the proposed algorithm in building environments. To investigate the energy effectiveness, we use the energy consumption model as follows:

$$\begin{aligned}
&\boldsymbol{E} = \boldsymbol{E_S} + \boldsymbol{E_R}\\
&\boldsymbol{E_S} = \left[\boldsymbol{C^i_{TX}} \cdot \boldsymbol{T_{DATA}} + \boldsymbol{C^i_{TX}} \cdot \left(\boldsymbol{T_{LIFS}} + \boldsymbol{T_{SIFS}} + \boldsymbol{T_{ACK}}\right)\right] \cdot \boldsymbol{V}\\
&\boldsymbol{E_R} = \left[\boldsymbol{C^i_{TX}} \cdot \boldsymbol{T_{ACK}} + \boldsymbol{C_{RX}} \cdot \left(\boldsymbol{T_{LIFS}} + \boldsymbol{T_{SIFS}} + \boldsymbol{T_{DATA}}\right)\right] \cdot \boldsymbol{V} \quad (11)
\end{aligned}$$

where E_S and E_R denote the energy consumption for the sender and the receiver respectively. C^i_{TX} and C_{RX} denote the current consumption for the transmitting with the transmit power level *i* and the receiving. T_{DATA}, T_{ACK}, T_{LIFS}, and T_{SIFS} denote the durations of the data packet, the ACK packet, the long inter-frame space, and the short inter-frame space respectively [1]. *V* denotes the voltage supply value for the radio module.

As shown in Fig. 8, we randomly deploy 150 nodes in 200 x 150*m* space. We use the multi-wall model which is the semi-empirical propagation model [19]. The distance-based algorithm is the RNG with the distance. The RSSI-based algorithm is the XTC that constructs the RNG with the RSSI. As shown in Fig. 8-(d), the proposed algorithm removes the links that are affected by the interference.

TABLE I
SIMULATION RESULTS

algorithm	number of hops	delivery rate (%)	energy consumption (uJ/Byte)
distance-based	7	11.88	118.37
RSSI-based	9	29.72	82.37
proposed	13	79.66	63.42

To see the advantage of the proposed algorithm with the routing protocol, we randomly choose two nodes and establish the shortest route over the constructed topology. Table 1 shows the averaged performance of the proposed algorithm and other algorithms. The proposed algorithm shows good performance results in terms of the delivery rate and the energy consumption. The reason is that the proposed algorithm detours the messages around the interference region, but other algorithms forward the messages through the interference region. Other algorithms consume a lot of energy to retransmit the messages due to packet transmission failures.

B. *Testbed Experiment Results*

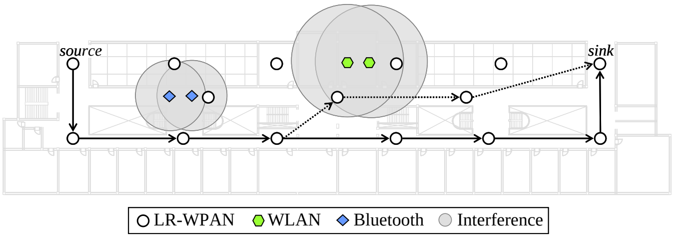

Fig. 9. Experiment scenario of the proposed algorithm under high (or low) traffic rate WLAN interferences.

To see the effectiveness of the proposed algorithm, we also conducted testbed experiments with LR-WPAN (MTM-CM3000), WLAN (N200UA), and Bluetooth (BTD201M) devices. The MTM-CM3000 has the CC2420 IEEE 802.15.4 radio and the N200UA has the RT2870 IEEE 802.11a/b/g/n radio [17][18]. The WL-BTD201M has the BCM2045 IEEE 802.15.1 radio and the integrated PCB antenna [20]. As shown in Fig. 9, we place 15 LR-WPAN, 2 WLAN, and 2 Bluetooth devices on the 5th floor of the building. In the experiments, the LR-WPAN nodes construct the topology and then, the source node transmits 50-byte messages to the sink node through the route at a rate of 1 packet per second. In the meanwhile, the one Bluetooth node streams the music to the other Bluetooth node.

We first perform the experiments under the low traffic rate WLAN interference. In the experiments, one WLAN node randomly accesses the Web sites through the WLAN AP. Table 2 shows the performance of the proposed algorithm and other algorithms under the low-traffic-rate WLAN interference. The proposed algorithm has the same number of hops to the RSSI-based algorithm, but it shows higher delivery rate and lower energy consumption. The proposed algorithm does not change the topology, it compensates the transmit power to keep the good link quality.

TABLE II
EXPERIMENTAL RESULTS UNDER LOW TRAFFIC RATE WLAN INTERFERENCE

algorithm	number of hops	delivery rate (%)	energy consumption (uJ/Byte)
distance-based	5	46.79	55.25
RSSI-based	6	68.84	52.13
proposed	6	83.32	32.85

TABLE III
EXPERIMENTAL RESULTS UNDER HIGH TRAFFIC RATE WLAN INTERFERENCE

algorithm	number of hops	delivery rate (%)	energy consumption (uJ/Byte)
distance-based	5	14.62	99.40
RSSI-based	6	33.49	58.55
proposed	7	76.02	40.21

We next perform the experiments under the high traffic rate WLAN interference. In the experiments, one WLAN node downloads a big file from another WLAN node through the file transfer protocol (FTP). As shown in table 3, the proposed algorithm has the longest route because it has re-constructed local topology adaptively to avoid wireless links affected by WLAN interference. The proposed algorithm is superior to other algorithms in terms of the delivery rate and the energy consumptions because it removes wireless links corrupted by interferences and detours the messages around the interference region.

TABLE IV
PHYSICAL NODE DEGREE

algorithm	under congested interference	under uncongested interference
distance-based	3	3
RSSI-based	4	3
proposed	6	4

Table 4 shows the average physical node degree of algorithms. The physical node degree is the number of neighbors that are within the transmission range of the node. The physical node degree of the proposed algorithm is slightly larger than the other algorithms. The reason is that the proposed algorithm increases the minimum transmit power according to the interference power level. In fact, the contention and the energy consumption can be increased as the physical node degree increases. However, the proposed algorithm can compensate this disadvantage by minimizing the interference effects.

VI. CONCLUSIONS

The LR-WPANs can suffer the significant performance degradation due to the 2.4GHz interferences such as WLAN or Bluetooth devices. In this paper, we propose the interference-aware topology control (ITC) algorithm for the LR-WPANs. We determine the minimum-transmit-power based on the interference effect analysis. Each node estimates the interference effects periodically and re-constructs the network topology when interferences are detected. The re-constructed topology reduces the various interference effects and increases the network performance significantly. We evaluate the performance of the proposed algorithm with simulations and real wireless platforms. From various performance results, we confirm that the proposed algorithm is robust to the 2.4GHz interference effects and improves the network performance with a routing protocol.

REFERENCES

[1] *Part 15.4: wireless medium access control (MAC) and physical layer (PHY) specifications for low-rate wireless personal area networks (LR-WPANs)*, IEEE std. 802.15.4, 2006.
[2] *Zigbee specification, Zigbee std., 2006.*
[3] *Part 11: wireless LAN medium access control (MAC) and physical layer (PHY) specifications,* IEEE std. 802.11, 2007.
[4] *Part 15.1: wireless medium access control (MAC) and physical layer (PHY) specifications for wireless personal area networks (WPANs)*, IEEE std. 802.15.1, 2005.
[5] P. Santi, “Topology control in wireless ad hoc and sensor networks,” *ACM computing survey*, vol. 37, no. 2, pp. 164-194, 2005.
[6] K. Gabriel and R. Sokal, “A new statistical approach to geographic variation analysis,” *Systematic Zoology*, vol. 18, pp. 259-278, 1969.
[7] J. Jaromczyk and G. Toussaint, “Relative neighborhood graphs and their relatives,” in *Proc. IEEE*, vol. 80, no. 9, pp. 1502-1517, Sep. 1992.
[8] A. Yao, “On constructing minimum spanning trees in k-dimensional spaces and related problems,” *SIAM J. Comput.*, vol. 11, pp. 721-736, 1982
[9] Li Li, J. Halpern, P. Bahl, Y. Wang, and R. Wattenhofer, “A cone-based distributed topology-control algorithm for wireless multi-hop networks,” *IEEE Trans. Networking*, vol. 13, no. 1, Feb., 2005.
[10] S. Borbash and E. Jennings, “Distributed topology control algorithm for multihop wireless networks,” in *Proc. IJCNN*, pp. 355-360, Honolulu, HI, 2002.
[11] R. Wattenhofer and A. Zollinger, “XTC: a practical topology control algorithm for ad-hoc networks,” in *Proc. WMAN*, Santa Fe, NM, USA, 2004.
[12] M. Dyer, J. Beutel, and L. Thiele, “S-XTC: a signal-strength based topology control algorithm for sensor networks,” in *Proc. ISADS*, Sedona, AZ, USA, Mar., 2007.
[13] G. Hackmann, O. Chipara, and C. Lu, “Robust topology control for indoor wireless sensor networks,” in *Proc. SenSys*, Raleigh, NC, USA, Nov., 2008.
[14] M. Petrova, L. Wu, P. Mahonen, and J. Riihijarvi, “Interference measurements on performance degradation between collocated IEEE 802.11g/n and IEEE 802.15.4 networks,” In *Proc. ICN*, Sainte-Luce, Martinique, Apr., 2007.
[15] N. Golmie, O. Rebala, and N. Chevrollier, “Bluetooth adaptive frequency hopping and scheduling,” In *Proc. MILCOM*, vol. 2, pp. 1138-1142, Boston, MA, USA, Oct., 2003.
[16] R. Musaloiu-E and A. Terzis, “Minimizing the effect of wifi interference in 802.15.4 wireless sensor networks,” *Int. J. Sensor Networks*, vol. 3, no. 1, 2008.
[17] S. Han, S. Lee, S. Lee, and Y. Kim, “Coexistence performance evaluation of IEEE 802.15.4 under IEEE 802.11b interference in fading channels,” in *Proc. PIMRC*, Athens, Greece, Sep., 2007.
[18] S. Shin, H. Park, S. Choi, and W. Kwon, “Packet error rate analysis of zigbee under wlan and bluetooth interference,” *IEEE Trans. Wireless Commun*. Vol. 6, no. 8, pp. 2825-2830, Aug., 2007.
[19] S. Zvanovec, P. Pechac, and M. Klepal, “Wireless LAN networks design: site survey or propagation modeling?,” *Radioengineering*, vol. 12, no. 4, Dec., 2003.
[20] A. Sampath, P. Kumar, and J. Holtzman, “On setting reverse link target SIR in a CDMA system,” in *Proc. VTC*, pp. 929-933, Phoenix, USA, May, 2007.

[21] K. Srinivasan, P. Dutta, A. Tavakoli, and P. Levis, "Understanding the cause of packet delivery success and failure in dense wireless sensor networks," in Proc. Sensys, Boulder, CO, Nov., 2006.

[22] T. Rappaport, *Wireless communications: principles and practice*, 2nd ed., Prentice Hall PTR, 2002, pp. 105-168.

[23] *CC2420 2.4GHz IEEE 802.15.4 / zigbee RF transceiver*, Chipcon, 2003.

[24] *RT2800 MIMO wireless chipset family*, Ralink, 2007.

[25] *Titanis 2.4GHz swivel SMA antenna*, Antenova, 2007.

[26] *BCM2045 blutonium bluetooth 2.0 + EDR single-chip HCI solution*, Broadcom, 2007.

Junseok Kim received the B.S degree in Electronic Engineering from Konkuk University, Seoul, Korea, in 2008. He is now master student in Konkuk University and he is a member of the wireless and mobile networking (WIMNET) lab.

Younggoo Kwon received the B.S and M.S degrees in Electrical Engineering from Korea University, Seoul, Korea, in 1993 and 1996, respectively, and the Ph.D. degree in Electrical Engineering from the Department of Electrical and Computer Engineering, University of Florida, Gainesville, in 2002. From 2002 to 2003, he was a Senior Member of the Research Staff at Samsung Electo-Mechanics Central R&D Center. Currently, he is an Assistant Professor in the Department of Electronics Engineering, Konkuk University, Seoul, Korea.